

Phase transitions and critical phenomena of tiny grains thin films synthesized in microwave plasma chemical vapor deposition and origin of ν_1 peak

Mubarak Ali ^{a, *} and I-Nan Lin ^b

^a Department of Physics, COMSATS Institute of Information Technology, Islamabad 45550, Pakistan.

^b Department of Physics, Tamkang University, Tamsui Dist., New Taipei City 25137, Taiwan (R.O.C.).

*corresponding address: mubarak74@comsats.edu.pk, mubarak74@mail.com, Ph. +92-51-90495406

Abstract –Different trends have been observed in Raman spectroscopy and field emission characteristics of tiny grains carbon films known as nanocrystalline and ultra-nanocrystalline diamond films. Carbon atoms when in solid-state evolve several structural phases of deposited film depending on the dynamics of atoms. Those tiny grains of carbon film evolved graphite phase of structure and followed the uniform elongation of atoms modified into structure of smooth elements, which revealed the origin of ν_1 peak in the Raman spectrum. The tiny grains retained two-dimensional structure in the film become the origin of ν_2 peak. Where tiny grains or their atoms originate ν_1 peak, it is at low intensity as compared to the ones known in their exceptional hardness because of different positions of electron states at bare surface of their atoms depend on the process of synergy. Enhanced field emission characteristics of films resulted is because of the tiny grains modified structure into structure of smooth elements where accelerating of propagation of photonic current is resulted. On interacting laser beam to tiny grains carbon film comprised different phases intensity of signals recorded at different wave numbers revealing the same trend as for energy bands in their energy loss spectroscopy.

Keywords: Tiny grains carbon films; Force energy; Heat energy; Phase transitions; Raman spectra; Energy loss spectroscopy; 2D Materials

1.0 Introduction

Phase transition of atoms of suitable electronic transitions is crucial as it may be the origin of a new phenomenon. Development of selective size and shape materials and investigating their characteristics at nano and atomic scale requires a new sort of observations. Wherever dynamics influence the process evolution of structure in different phases may be anticipated even though the comprised atoms belong to the same element. When carbon atoms transforming into certain solid-state behavior evolving structure they might undergo various sorts transformations owing to several available options of electron-dynamics. Moreover, regulating structure of carbon atoms in certain positions of electron states may deal the specific modification. Additionally, depending on the process conditions and employed technique of the synthesis atoms might differ in their transformation and modification behaviors. In hot-filaments chemically deposited carbon, tiny grains are made as well prior to go for sticking at substrate and may influence the phase of evolving structure of grains and crystallites resulting into switch phase [1].

The syntheses of nanocrystalline diamond (NCD) and ultrananocrystalline diamond (UNCD) films only span over few decades where interplay of varying process conditions in the presence of different concentrations of feed gases (methane, hydrogen and argon, etc.) while employing technique known as microwave plasma chemical vapor deposition (MPCVD) are the source of their development. The performances of NCD/UNCD films are mainly recognized in terms of their microscopic observations, Raman and energy loss spectroscopic analyses and field emission characteristics. The NCD/UNCD films mainly deal tiny grains, size range in tens of nanometer to few nanometers.

It is necessary to understand dynamics of tiny particles' formation prior to go for assembling into large size particles [2]. Agglomerations of colloidal matter envisage atoms and molecules to deal them as materials for tomorrow [3]. Dynamics of formation of different tiny particles have been discussed elsewhere [4]. The formation mechanism of tiny shaped particles under certain concentration of gold precursor has been discussed [5]. Under identical process parameters, the nature of precursor directs tiny shaped particles following by large shaped particles where role of atomic nature is crucial [6]. Different tiny shaped particles were developed under the 'tailored energy-shape photons' while varying the ratio of bipolar pulse OFF to ON time [7]. Triangular-shaped tiny particles synthesized directly under unipolar

pulse ON/OFF time and a certain structure evolved under the combined application of characteristic photon and a field force behavior [7]. Formation process of large-sized particles reveals very high development rate and tiny-sized particles which didn't attain uniform drive deal diffusion prior to gain their perfect fit and compact packing [8]. A monolayer tiny particle in connecting triangles is under the tailored energy photon shape like tiny particle itself where it divides into two equal triangular-shaped tiny particles under the application of field force [5-8]. In all suitable metals and semimetals, the binding of atoms takes place under the construction of energy knots made by the coupling of unit photons (a force energy-directed phenomenon) [9]. Tiny shaped particle dealing localized gravity at solution surface along with modification of structure to structure of smooth elements have been discussed elsewhere [10]. Atoms of suitable elements execute electronic transitions don't ionize, deform or elongate while inert gas atoms split under the application of photonic current [11]. The phenomena of heat and photon energy have been discussed while dealing silicon atom where under confined electron-dynamics energy is being transformed into force energy [12]. Atomic binding in diamond-diamond state is a force-directed phenomenon while graphitic-graphitic state is an almost neutral force-directed phenomenon instead of force energy-directed phenomenon [13]. Under normal conditions, certain nature atoms of tiny particles deal deformation and elongation behaviors at greater extent along with field force behavior which may work either effective nanomedicine or defective [14].

Electron field emission (EFE) device fabricated by heating tiny diamond grains in hydrogen plasma reveals high characteristic and is due to high defect density and low electron affinity [15]. Increasing nitrogen content slightly increases sp^2 -bonding in grain-boundary and local bonding structure remains the same [16]. Diverse geometries coupled with varieties of attachment sites enabling diamondoids as useful building blocks for molecular-design applications [17]. Size of grains in UNCD film in the range of 2-3 nm remains thermodynamically stable as tested under broad range of pressure –temperature of hydrogenated surfaces [18]. Grains in nanometer size indicate specific changes because of the decreased mobile dislocations and below their critical size, a softening behavior is often observed and change is triggered by atomic shuffling where simulations approaches are incapable to evaluate underlying mechanism [19]. Sumant *et al.* [20] investigated the surface

chemistry and nanotribology inside the UNCD films and are indistinguishable chemically, adhesively and tribologically from single-crystal diamond.

Several studies of UNCD films are available in the literature targeting field emission characteristics under different process parameters along with varying concentration of gases (and dopants as well). On increasing the local density of states UNCD films provide conducting path at diamond-vacuum interface [21]. UNCD films synthesized at low temperatures and in nitrogen environment demonstrated high conductivity in their various applications [22]. Under nitrogen atmosphere, the grain size of UNCD film becomes smaller than 10 nm and metallic conductivity is achieved [23]. UNCD film has low friction/wear and rapid passivation of dangling bonds is a matter of concern in humid environment [24]. UNCD films are different as compared to NCD films in several ways such as their grain sizes are 2 nm to 5 nm, they are bound by sp^2 -carbon and usually grow in argon-rich/hydrogen-poor CVD environment and may contain 95–98% sp^3 -bonded carbon [25]. In UNCD films, homojunction facilitates the tunneling of electrons in conduction band and their direct transport at conducting/insulating interface [26]. To synthesize diamond films at temperatures below 600°C, UNCD films are superior in choice because their properties don't degrade as in polycrystalline diamond films [27]. On increasing substrate temperature along with hydrogen concentration in Ar/CH₄ plasma, sp^3 -diamond phase becomes less passivated [28]. Low friction coefficient of UNCD films is linked with large amounts of hydroxylic/carboxylic functional groups which are recognized as grain boundary [29]. Bias enhanced nucleation/growth processes facilitate the transport of graphitic phase in both interior and interface regions of UNCD films [30]. Hydrogen concentration increases the size of diamond grains [31]. Boron-doped UNCD films are capable of being utilized in the field of atomic force microscopy/robust electrodes/bio-compatible sensors [32]. On lowering the a-C layer at interface UNCD/Au-Si composite structure delivers better conductivity and improves EFE [33]. Precise growth of sub-2 nm/above 5 nm sized diamond grains is achieved due to energetic species under low growth temperature and pre-nucleated interface, thus, tiny grains on silicon nanoneedles deliver enhanced EFE [34]. Gold-UNCD films show superior EFE properties than copper-UNCD films and authentic factor underneath the mechanism is the presence of nanographitic phases [35]. Copper ion implantation and annealing process increase the EFE due to improved conducting nature of UNCD films [36]. Presence of graphitic phases at the interfaces

of ZnO nanorods/UNCD needles decreases the resistivity of layer and core-shell heterostructures, thus, delivered superior EFE [37]. Nitrogen-incorporated UNCD grains serve as 'high-density diamond nuclei' in the hybrid carbon film [38]. In all the above studies and many others not cited here, factors related to performance of UNCD/NCD films are linked with the tiny grains of UNCD/NCD films. Improvement in the conductivity but not EFE of P-ions incorporated-UNCD films was due to the transportation of electrons crossing interface [39]. Transportation of electrons is the prime reason for enhanced conductivity and emission properties of doped UNCD films [40].

In various studies of NCD/UNCD films where high-resolution microscopic studies conducted, atoms of tiny grains reveal elongation as well as deformation behaviors and it is hard to recognize their atoms in real shape. Again, various Raman spectra and energy loss spectroscopic analyses of 'tiny grains carbon films' reveal different peaks of varying intensity along with their different trend. Additionally, a film synthesized under the same parameters show different information of obtained data at different locations. Those indicates that 'tiny grains carbon films' deal miscellaneous behaviors of their structure where in addition to graphite structure, modified and transformed structures accompanied too jointly determining a certain characteristic of the deposited carbon film.

In the present work, different 'tiny grains carbon films' known as NCD and UNCD films are synthesized in MPCVD. Formation process of 'tiny grains carbon films' is discussed under the variation of chamber pressure and different concentration of hydrogen gas. Different structures, their modification and transformations of in other structures discussed. Raman spectroscopy and energy loss spectroscopy of 'tiny grains carbon films' tally each other along with their field emission characteristics. The performance of carbon films in terms of modified tiny grains to structure of smooth elements is pinpointed. In addition to those, confusion has been going on since three decades regarding the origin of peak related to ' ν_1 band' in Raman spectra and it was due to the size of the grains or the presence of transpolyacetylene layers around tiny grains. Present study indicates the real reason of the peak related to ' ν_1 band'. Again, position of electron states at bare surface of carbon atom in each case of its transformation to different state is located; lonsdaleite, fullerene (bucky balls), nanotube and graphene along with binding of graphene-graphene state

atoms. The Mohs hardness of carbon atoms (nanoscale materials) under different levity gravity behaviors of electron states is also sketched.

2.0 Experimental details

To synthesize 'tiny grains carbon films', MPCVD technique (IPLAS-Cyrannus, 2.45 GHz) was employed. A schematic of MPCVD set up have been shown elsewhere [41]. Silicon wafers N-type nature, resistivity $\sim 1-5$ (Ohm-cm), were used as the substrate material. Initial duration of the process (at nucleation stage) was set 30 minutes, whereas, deposition time was set 60 minutes, in each experiment. Prior to loading the samples in the chamber, substrates were cleaned by ultrasonic agitation for the duration of 30 minutes in methanol solution containing nanodiamond powders size ~ 30 nm and titanium powders of 325 mesh to create nucleation sites. The total mass flow rate was 200 sccm and was kept constant in each experiment. The substrate temperature was measured by K-type thermocouple where 6 % H₂ in argon –rich methane mixture was used to synthesize carbon films and the recorded value was $700^{\circ}\text{C}\pm 10^{\circ}\text{C}$, whereas, the temperature was significantly lowered in films synthesized without H₂ where recorded value was $500^{\circ}\text{C}\pm 10^{\circ}\text{C}$. On increasing chamber pressure from 100 torr to 200 torr at constant microwave power 1400 (watts), no remarkable difference in temperature was noted. Due to lower thermal conductivity of Ar than H₂, heating of substrate by plasma is greatly reduced in argon-rich CH₄ mixture [22]. Surface morphology of 'tiny grains carbon films' were analyzed by scanning microscope (FE-SEM, ZEISS, Model: SIGMA). Peaks related to different phases of carbon were identified by Raman spectroscopy (Renishaw; 325 nm and HR800 UV; 632.8 nm). Photon field emission (PFE) characteristics known as electron field emission characteristics of 'tiny grains carbon films' were deduced by using a tunable parallel plate set-up known in $I - V$ curve and measurements were made by employing an electrometer (Keithley 237) under vacuum level of 10^{-6} torr. Dark field, bright field, high-resolution images and selected area photon reflection (SAPR) patterns (known as SAED patterns) of 'tiny grains carbon films' were taken by high-resolution transmission microscope (HR-TEM, JEOL JEM2100F) operated at 200 kV. Energy of different bands in 'tiny grains carbon films' was deduced by core loss photon energy loss spectroscopy (core loss PELS) and low loss photon energy loss spectroscopy (low loss PELS) known as core loss EELS and low loss EELS.

3.0 Results and discussion

Surface morphology of carbon films of various size and shape of tiny grains synthesized at different chamber pressures are shown in Figures S1 (a) to S1 (c); at 150 torr, more tiny grains are in needle-like shapes. In films synthesized at 100 torr and 200 torr, tiny grains are composed more like in the shape of tiny clusters. Morphological features of tiny grains in film synthesized without H₂ gas (Figure S2) are like the ones in film synthesized at 6 % H₂ (Figure S1b). Raman spectra of different films synthesized at 100 torr, 150 torr and 200 torr are shown in Figure 1 revealing different intensity levels of peak related to 'ν₁ band'. The 'ν₁ band' in films synthesized at 100 torr and 200 torr is more pronounced as compared to the film synthesized at 150 torr. The 'ν₁ band' is intensive in film synthesized without H₂ gas (Figure S3) as compared to the films synthesized at 6% H₂ (Figure 1). In different Raman spectra, the peak related to 'ν₁ band' is at low level of intensity as compared to D*, D and G peaks. Field emission current density (in known units) as a function of applied field (in known units) at various chamber pressures is shown in Figure 2. Film synthesized at 100 torr shows superior field emission properties where 'turn on field' is 11.52 V/μM (the lowest value) and the large current density (> 2.0 mA/cm²). The 'turn on field' was the highest (25 V/μM) in the film synthesized at 150 torr, whereas, it is recorded 16.4 V/μM at 200 torr.

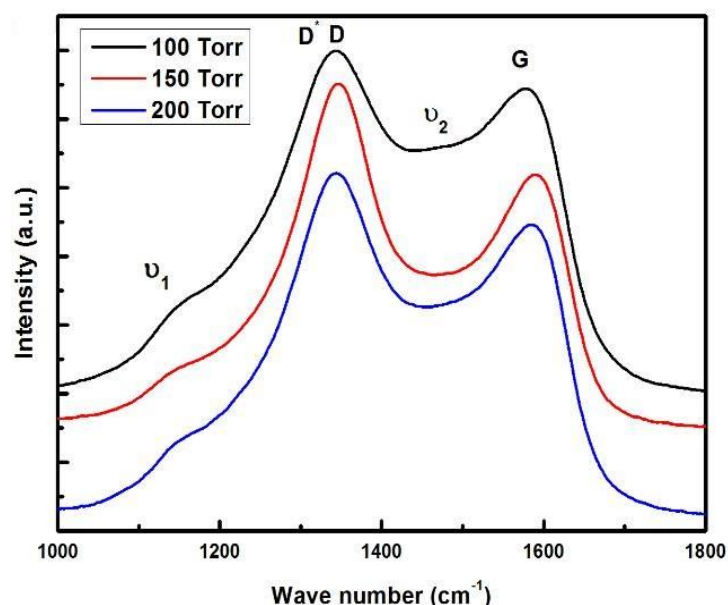


Figure 1: Raman spectra of 'tiny grains carbon films' synthesized at chamber pressure 100 torr, 150 torr and 200 torr; total mass flow rate: 200 sccm (6% H₂, 1 % CH₄ and 93 % argon, Ar: CH₄: H₂ = 186:2:12), microwave power: 1400 (in watts) and deposition time: 60 minutes.

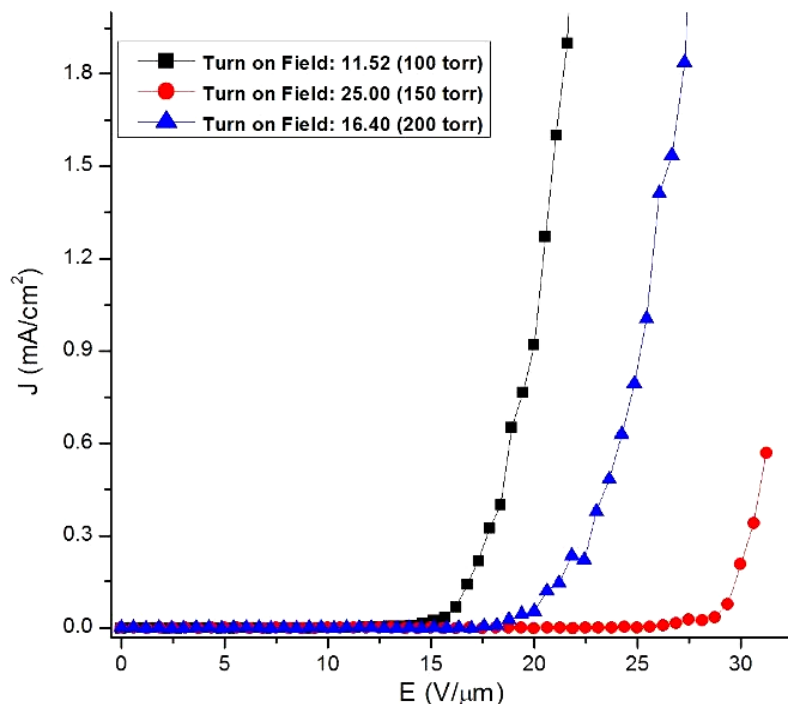


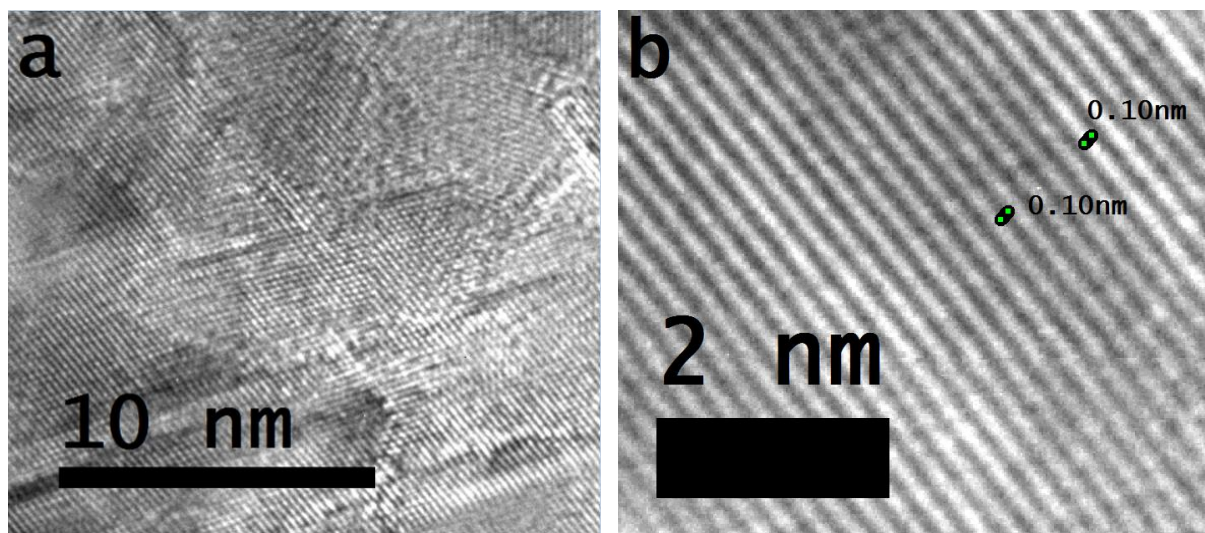
Figure 2: Field emission current density of ‘tiny grains carbon films’ synthesized at chamber pressure 100 torr, 150 torr and 200 torr as a function of applied field; total mass flow rate: 200 sccm (6% H₂, 1 % CH₄ and 93 % argon, Ar: CH₄: H₂ = 186:2:12), microwave power: 1400 (in watts) and deposition time: 60 minutes.

Field emission current density of different ‘tiny grains carbon films’ synthesized in Ar-rich CH₄ mixture without H₂ and with H₂ (3% and 6%) as a function of applied field are shown in Figures S4 (a-c). In Figures S4 (a) to S4 (c), the general trend of the ‘turn on field’ is more morphology-dependent; the value of ‘turn on field’ at 100 torr is lower than that at 150 torr (same trend in Figure 2). Under lower chamber pressure (at 100 torr) all films in Figure S4 (a-c) show lower ‘turn on field’ where more number of tiny grains modified structure to structure of smooth elements as low ‘turn on field’ value was measured due to enhanced and accelerated propagation of photonic current, whereas, the large value of ‘turn on field’ in film synthesized at 200 torr (Figure S4a) is appeared to be related to modification of structure of less number of tiny grains to structure of smooth elements.

Dark field transmission microscope images of ‘tiny grains carbon films’ synthesized at 100 torr and 200 torr are shown in Figures S5 (a) and S6 (a) where small-sized dark spots are related to isolated tiny grains and bigger dark spots are related to coalesced (packed) tiny grains and contrast is more visible in bright field transmission microscope images shown in Figures S5 (b) and S6 (b); in some regions of the film, tiny grains amalgamated and in some regions of the film, tiny

grains dispersed. SAPR patterns taken at the same regions of films (shown in Figures S5b and S6b) are shown in Figures S5 (c) and S6 (c) where intensity spots don't show precise rings related to graphite structure and spotted intensity spots in the pattern reveal structure of different state atoms in 'tiny grains carbon films'. As indicated in the marked scale which is nearly a half of the nanometer where photons reflected at the surface of mixed behavior structure don't reveal any specific order in spotted dots of their intensity in both the patterns.

High-resolution transmission microscope image taken from 'tiny grains carbon film' synthesized at 100 torr is shown in Figure 3 (c) and from the figure, two regions of magnified images are shown in Figures 3 (a) and 3 (b). In Figure 3 (c), several tiny grains show modification of their structures to structure of smooth elements as they developed initially into graphite structure –a two-dimensional structure termed as master structure. In the image shown in Figure 3 (a), the most of underlying tiny grains (also those at the surface) appear to modify structures to structure of smooth elements. In Figure 3 (b), a single tiny grain is shown modified structure to structure of perfect smooth elements. The insert in Figure 3 (c) shows spectral analysis of the modified structure (taken from the structure of smooth elements shown in Figure 3b), which again reveals that where tiny grains made two-dimensional structure (graphite structure or master structure) modified structures to structure of smooth elements.



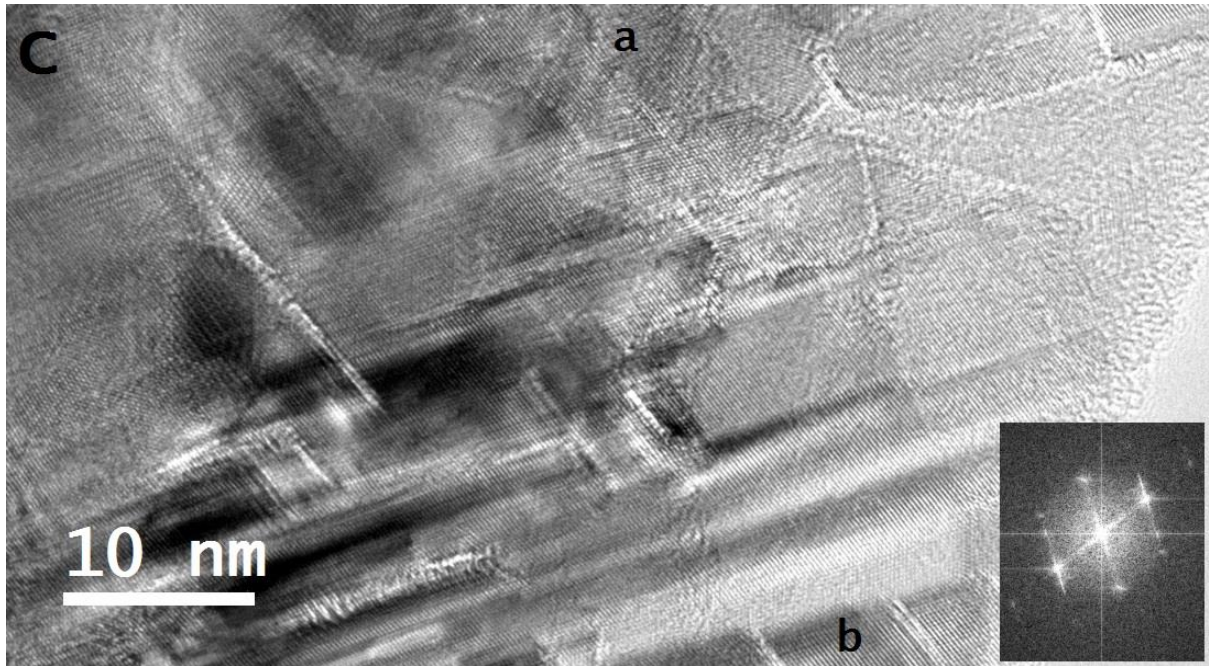


Figure 3: (a) Magnified view of the selected region of high-resolution transmission microscope image shows several overlaid tiny grains, (b) magnified view of the selected region of high-resolution transmission microscope image shows graphite structure tiny grain modified structure to structure of smooth elements and (c) standard high-resolution transmission microscope image shows large number of tiny grains modified structures to different structures; ‘tiny grains carbon film’ synthesized at chamber pressure: 100 torr, mass flow rate: 200 sccm (6% H₂, 1 % CH₄ and 93 % argon), microwave power: 1400 (in watts) and deposition time: 60 minutes.

Figure S7 shows high-resolution transmission microscope image taken from another region of the carbon film, which highlights different features of the tiny grains. Gap between two structures of smooth elements labeled by (2) indicates formation of canal-like channel which is referred as ‘graphitic filament’ [39, 41]. High-resolution transmission microscope image taken from the carbon film synthesized at 200 torr is shown in Figure 4 (c) revealing different structures of ‘tiny grains carbon film’ and two regions of magnified high-resolution transmission microscope images from the figure are shown in Figures 4 (a) and 4 (b). In Figure 4 (a), the tiny grains are in graphite structure but in Figure 4 (b), a tiny grain elongated and modified structure to structure of smooth elements under the field force of two opposite poles along with energy of travelling suitable wavelengths photons. A canal-like channel is formed between two tiny grains denoted by red dotted line in Figure 4 (b) where they modified structures to structure of smooth elements. The insert in Figure 4 (c) shows spectral analysis of ‘graphite structure tiny grain’ (which didn’t elongate as shown in Figure 4a) where spotted intensity spots of reflected photons also reveal two-

dimensional structure and it is not the case of inserted image in Figure 3 (c) as that reveals structure of smooth elements.

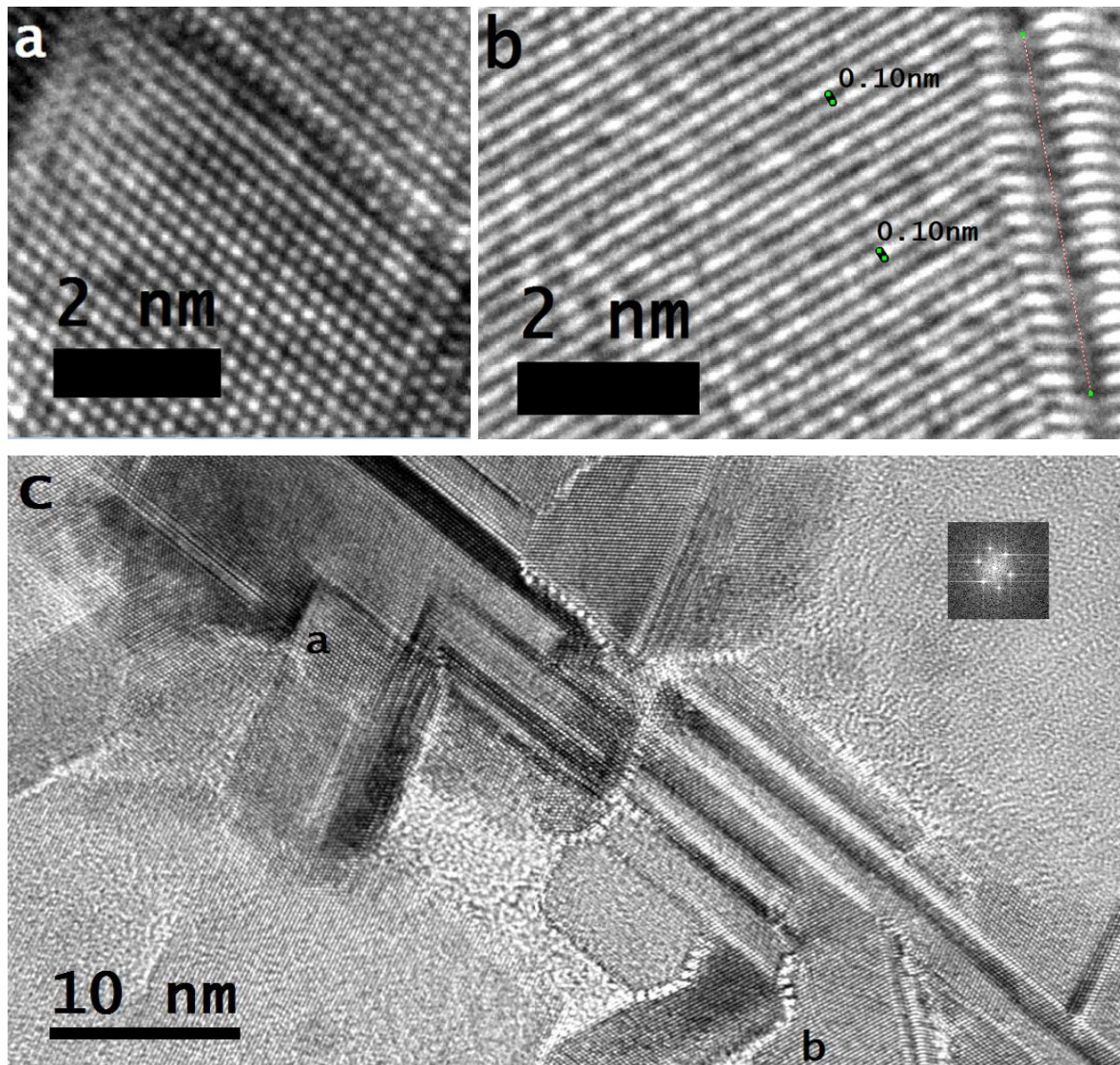


Figure 4: (a) Magnified view of the selected region of high-resolution transmission microscope image shows tiny grain of graphite structure, (b) magnified view of the selected region of high-resolution transmission microscope image shows modified tiny grain of graphite structure to structure of smooth elements and (c) standard high-resolution transmission microscope image shows several tiny grains where some are in graphite structure (as in the inserted image taken from magnified view of structure in 'a'), some tiny grains modified structures to structure of smooth elements and some retain other structures; 'tiny grains carbon film' synthesized at chamber pressure: 200 torr, mass flow rate: 200 sccm (6% H₂, 1 % CH₄ and 93 % argon), microwave power: 1400 (in watts) and deposition time: 60 minutes.

From these high-resolution microscopic images, it is difficult to identify transformed carbon atom of tiny grains into other states known in their exceptional hardness along with other specific features as different positions of electron states at

bare surface of their atoms are not differentiating. However, it is clear for tiny grains to evolve in graphite structure and deal uniform elongation behavior of atoms where their structures modify to structure of smooth elements. Again, where tiny grains of graphite structure don't deal any sort of elongation, they retain two-dimensional structure of their atoms. Here, 'electronic structure' is referred to that structure where electron states of atoms stretch, either orientationally or non-orientationally, thus, referred those atoms as 'elongated atoms' and in the case of uniform elongation of 'graphite structure tiny grain', it is referred to 'elongated tiny grain', such structure modify to structure of smooth elements under the field force of two opposite poles or/along with influence of travelling suitable wavelengths photons. In such 'carbon tiny grains films' propagation of photonic current is accelerated and enhanced because of the well-channelized inter-state electron's gap. This is the cause of recognition of UNCD/NCD films in terms of enhanced field emission characteristics where inter-state electron's gap works efficiently, thus, allowing propagation of accelerated current density of photons wavelength in inter-state electron's gap. This reveals that a tiny-sized particle or quantum dots (or the larger ones) evolve two-dimensional structure doesn't collectively oscillate on trapping or coupling light (photons) and photons of adequate wavelength on their surface in the case not utilize to align them under the impact of their force energy, they sink resulting into transformation to merged/squeezed photons which are related to heat energy as discussed elsewhere [12]. Thus, disregards the largely studied phenomenon of surface polaritons. In the case of elongation of atoms of metallic tiny particles and modification of their electronic structures into structure of smooth elements instead of disregarding surface polaritons phenomenon, a surface plasmons phenomenon is disregarded as discussed elsewhere [4, 10].

Core loss PEELS obtained at the same region of 'tiny grains carbon films' from where high-resolution transmission microscope images were taken as shown in Figures 5 (a) and (b). An abrupt rise near 292 eV referred to σ^* -band and a large dip near 305 eV referred to diamond phase [42, 43] and these bands are also found in the films synthesized at 100 torr and 200 torr as shown in Figures 5 (a) and (b). However, in our opinions the large dip curve in both films which is more indicative in the case of film synthesized at 200 torr (Figure 5b) is due to energy of band related to tiny grains modified structures to structure of smooth elements (~ 285 eV). The core loss PEELS of both films reveal the same energy peaks related to different bands

and identical trend to the one observed in the case of Raman spectroscopy. But in the case of Raman spectroscopy, the peaks' positions were at different wave numbers, whereas, in core loss PEELS the peaks' positions are at different energy bands; atoms (or their tiny grains) of films transformed into lonsdaleite, diamond and graphene states are at peak ~ 295 (eV), ~ 308 (eV) and ~ 328 (eV), respectively. Tiny grains remained in graphite phase reveal decreasing level of energy in the form of dip curve at band ~ 304 (eV) in both films as notable in Figures 5 (a) and (b). In Figures 5 (a), more pronounced as hump-like peaks at ~ 328 eV is due to more atoms (or tiny grains) of films transformed into graphene state.

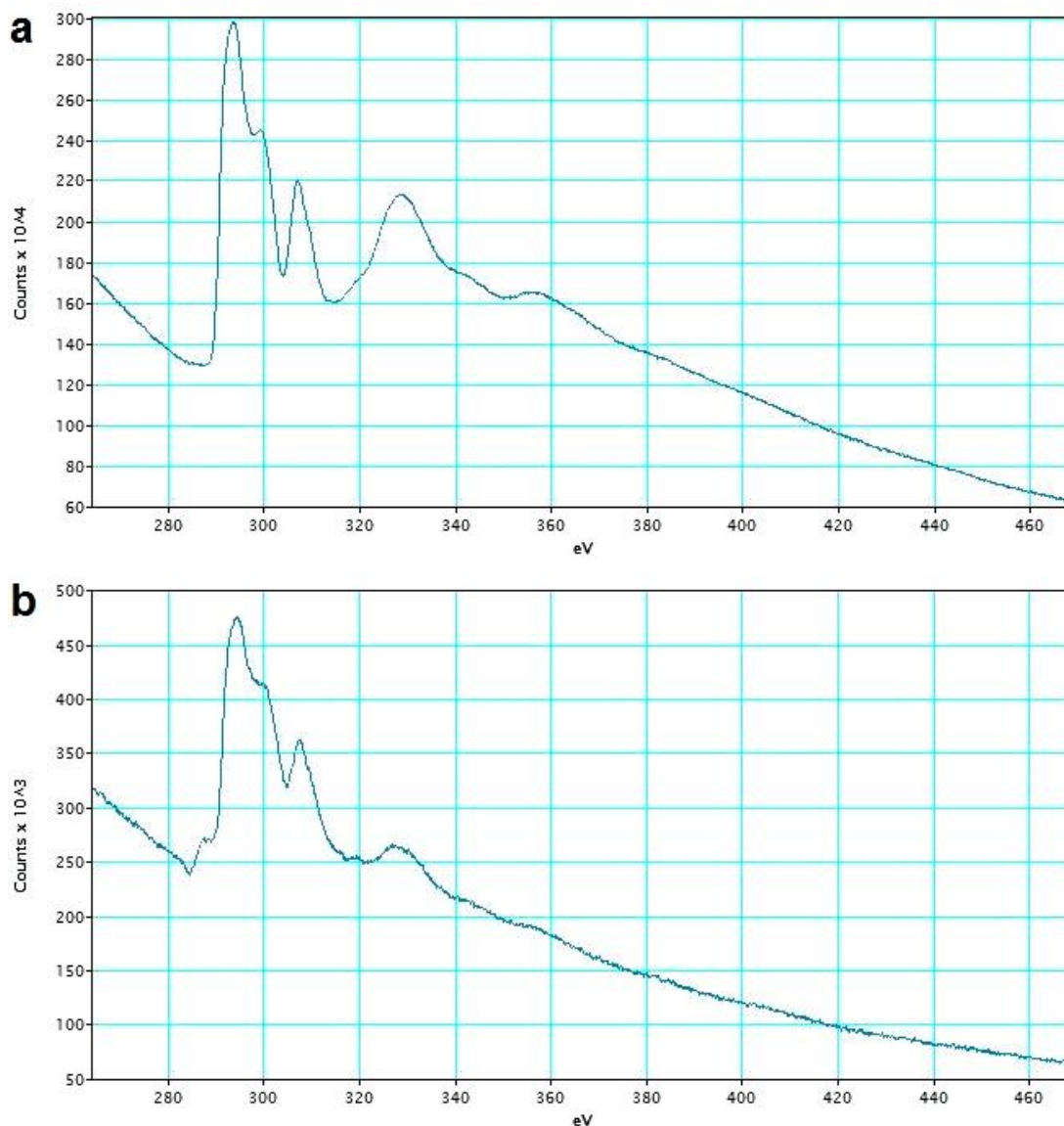


Figure 5: Core Loss photon energy loss spectroscopy (known as core loss EELS) of 'tiny grains carbon films' synthesized at chamber pressure (a) 100 torr and (b) 200 torr; total mass flow rate: 200 sccm (6% H₂, 1 % CH₄ and 93 % argon), microwave power: 1400 (in watts) and deposition time: 60 minutes.

In low loss EELS, graphite phase of carbon film shows a prominent peak at s_3 (27 eV), whereas, the a-C phase shows a peak at s_1 (22 eV) [43, 44]. However, in low loss PELS shown in Figures 6 (a) and (b), a peak at 27 eV is not available and band is at slightly tilted position instead of at 22 eV for both ‘tiny grains carbon films’ indicating different trend of phase transitions of tiny grains and different trend within these films. Overall, the trend of peaks’ behavior related to different band energy is in the same manner as observed in the case of core loss PELS of these films. The built-in unit (eV) in the case of core loss PELS and low loss PELS are replaced with photon volts (pV).

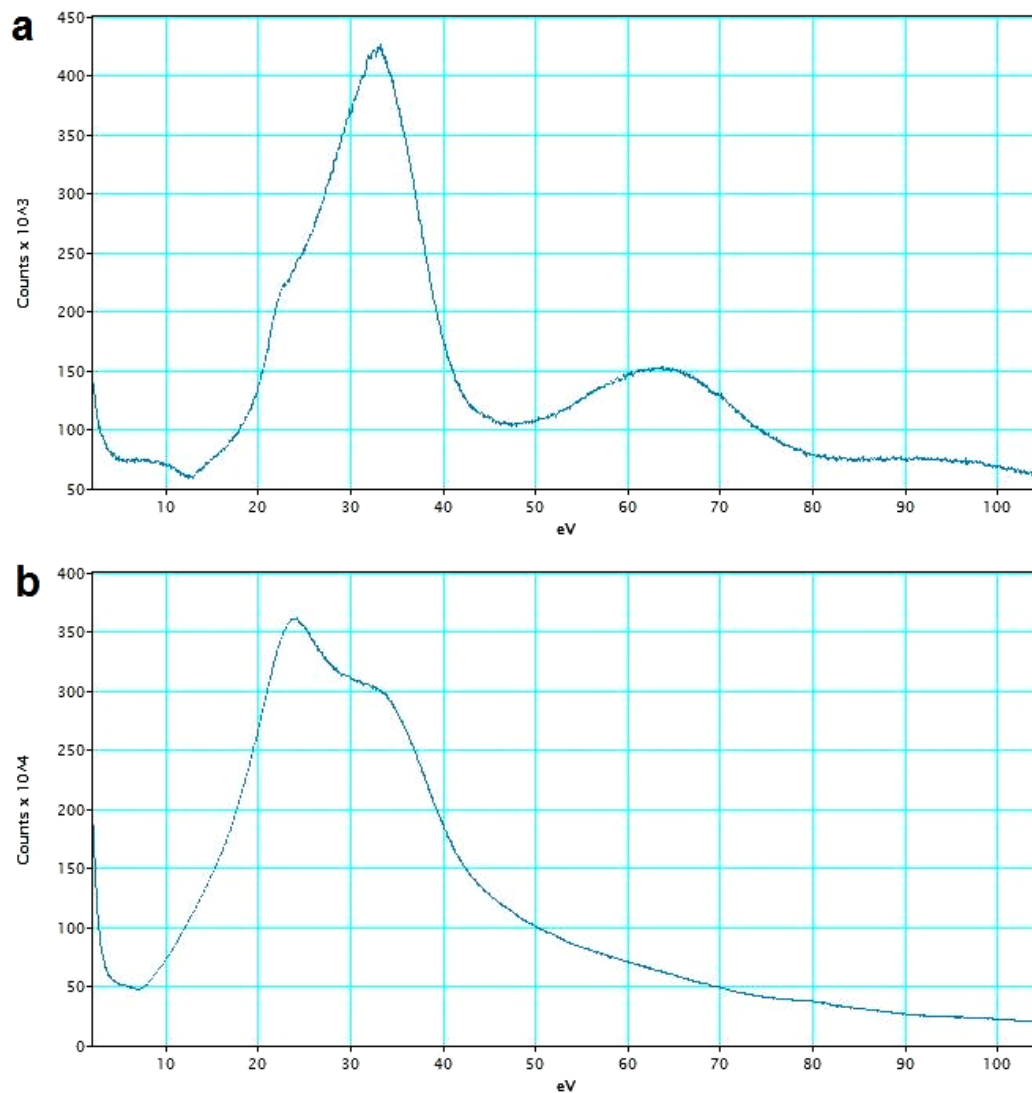


Figure 6: Low loss photon energy loss spectroscopy (known as low loss EELS) of ‘tiny grains carbon films’ synthesized at chamber pressure (a) 100 torr and (b) 200 torr; total mass flow rate: 200 sccm (6% H₂, 1 % CH₄ and 93 % argon), microwave power: 1400 (watts) and deposition time: 60 minutes.

In Raman spectra of NCD/UNCD films, the peak at 1150 cm^{-1} has been attributed to nanocrystalline diamond [44-46], however, the ν_1 peak (at 1150 cm^{-1}) cannot originate from a nanodiamond or related sp^3 -bonded phase but assigned to transpolyacetylene segments at grain boundaries and surfaces [47]. Nemanich *et al.* [45, 46] proposed that 1150 cm^{-1} peak arises from nanocrystalline or amorphous diamond. In the Raman spectrum of NCD/UNCD film, the sharp peak at 1332.1 cm^{-1} is the characteristic of diamond and broadening of the peak is related to the NCD grains [48]. In NCD/UNCD films, the peak at 1150 cm^{-1} appears hypothetically due to CH bonds and is always linked to another peak at 1450 cm^{-1} , and the peaks at 1330 cm^{-1} and 1560 cm^{-1} are due to D-band and G-band [49]. However, in the light of presented results of 'tiny grains carbon films', argon gas increased the rate of re-nucleation and the amount of tiny grains sizes $< 10\text{ nm}$ enhanced significantly. Depending on how many 'graphite structure tiny grains' modified structure to structure of smooth elements, their quantity experienced Raman laser, the contribution recorded in the form of peak at wave number $\sim 1150\text{ cm}^{-1}$. In microcrystalline diamond films, the size of grains is very large at large extent where they switch to another phase due to appreciable change in the localized conditions [1], thus, don't retain graphite structure and transformed into diamond state at large extent under the coordination of large amount of atomic hydrogen available in HFCVD reactor, accordingly, information put forth by Raman signals rather to record peak at 1150 cm^{-1} , the peak is recorded at 1332 cm^{-1} . Thus, the peak at wave number 1150 cm^{-1} is associated to those tiny grains developed in their graphite structure but modified structures to structure of smooth elements. Depending on the amount of modified graphite structure tiny grains the intensity of ' ν_1 peak' is varied; different intensity of ' ν_1 band' is related to the number of the tiny grains modified structures to structure of smooth elements under the Raman laser. Those tiny grains of graphite structure didn't elongate but retained two-dimensional structure which becomes the origin of ' ν_2 peak' in the Raman spectrum. In this way, wherever the ' ν_1 peak' is resulted in the Raman spectrum of carbon films the ' ν_2 peak' is resulted as well. Incorporating H_2 in Ar-rich CH_4 mixture either eliminates the ' ν_1 band' or it appears with less intensity. Without incorporation of H_2 in Ar-rich CH_4 mixture, peak related to ' ν_1 band' is pronounced as shown in Figure S3. On varying concentration of feed gases, the nature of tiny grains is varied as well, thus, counting different numbers of modified graphite structure tiny grains to structure of smooth elements

which record different intensity of ' ν_1 band' in the Raman spectrum. Again, different intensity of ' ν_1 band' is recorded on dealing Raman signals of different wavelength [50, 51] which is due to dealing varied levels of energy by modified graphite structure tiny grains in the same film.

In Raman spectroscopy, the peaks at different wave numbers are resulted because of propagating energy of interacting Raman laser in a different manner owing to different states of atoms (of tiny grains) in a carbon film as shown in Table 1; at wave number $\sim 1145 \text{ cm}^{-1}$, the peak (due to ν_1 band) is related to modified graphite structure tiny grains to structure of smooth elements and at wave number $\sim 1310 \text{ cm}^{-1}$, the peak (due to D^* band) is related to atoms (tiny grains) transformed into lonsdaleite state, and at wave number $\sim 1332 \text{ cm}^{-1}$, the peak (due to D band) is related to atoms (tiny grains) transformed into diamond state, and at wave number $\sim 1480 \text{ cm}^{-1}$, the peak (due to ν_2 band) is related to atoms (tiny grains) retained graphite structure and finally, at wave number $\sim 1580 \text{ cm}^{-1}$, the peak (due to G band) is related to atoms (tiny grains) of carbon film transformed to graphene state. In Table 1, wavelength of resulted Raman peaks related to different states of atoms is decreasing at increasing wave number indicating increase in the frequency under decreasing wavelength. In the case of ' ν_1 peak', the lowest energy of the structure resulted for modified graphite structure tiny grains to structure of smooth elements in the form of dip curve at ~ 285 (measured in eV) at core loss PELS, thus, gives the longest recorded wavelength ($\sim 8734 \text{ nm}$) in the Raman spectrum. On the other hand, where atoms (of tiny grains) transformed into graphene state, the highest energy of the structure resulted (~ 328 measured in eV) at core loss PELS, thus, gives the shortest wavelength in the Raman spectrum ($\sim 6329 \text{ nm}$). The tiny grains work under the lowest energy of the structure and the longest wavelength (shortest wave number) result into accelerated and enhanced propagation of photonic current as in the case of modified graphite structure tiny grains to structure of smooth elements, thus, their greater amount available in a carbon film results into enhance the field emission characteristics.

As it is tabulated in the Table 1, modified graphite structure tiny grains to structure of smooth elements give the highest value of wavelength indicating that they are the cause of enhanced field per unit length or area as discussed in the case of field emission characteristics of 'tiny grains carbon films'. In the case of lonsdaleite, diamond and graphene phases, the decreased values of wavelength are

resulted under the certain selection of rule set by rotated positions of electron states at bare surface of atoms, in each case. Now the question arises that recorded wavelength in the case of graphite structure is also between diamond and graphene (in Table 1) but measured hardness is at very low level, however, the peak related to graphite structure is at very low intensity in the Raman spectrum and we can observe that energy related to graphite structure is in the form of dip curve in the spectrum of photon energy loss spectroscopy. The scheme of electrons is different in atoms of graphitic state, modified structure and different transformed states of atoms, thus, delivered different response of the coordinated or interacted signals, which is distinctive in graphitic state and then in the case of modified structure and different transformed states of atoms in a ‘tiny grains carbon film’. Despite the fact, input energy entering ‘tiny grains carbon film’ was the same for atoms of graphitic state, modified structure and different transformed states but the resulting outcome varied as per structure. These findings solicit to devise science of Raman spectroscopy and energy loss spectroscopy, accordingly.

Table 1: Tiny grains carbon films record Raman peaks and energy peaks of tiny grains when modified graphite structure to structure of smooth elements, retain graphite structure (master structure), atoms transformed into lonsdaleite, diamond and graphene states at different wave numbers (cm^{-1}) and bands.

Tiny grain (s) modified structure to structure of smooth elements	Atoms (of tiny grains) in lonsdaleite state	Atoms (of tiny grains) in diamond state	Graphite structure (master structure)	Atoms (of tiny grains) in graphene state
Raman spectroscopy (in cm^{-1})				
$\nu_1 \sim 1145$ (8734 nm)	$D^* \sim 1310$ (7634 nm)	$D \sim 1332$ (7508 nm)	$\nu_2 \sim 1480$ (6757 nm)	$G \sim 1580$ (6329 nm)
Core loss photon energy loss spectroscopy (in eV)				
Dip curve at ~ 285	Peak at ~ 295	Peak at ~ 308	Dip at ~ 304	Peak at ~ 328

In MPCVD process, carbon atoms dissociated from the precursor at different rates resulting into attain different dynamics along with localized heating through which atomic bindings take place. In such cases, an atom can bounce back due to non-executing concurrent electron-dynamics at the instant of its amalgamation and the new comer may bind under different orientation of its executed electron-dynamics resulting into the evolution of mixed behavior (or amorphous) structure. In

the case of attaining uniform dynamics of atoms along with chasing the execution of concurrent electron-dynamics, it results into two-dimensional structure of tiny grain which is graphite structure and is also termed as master structure where almost a neutral force-directed phenomenon binds the atoms as discussed elsewhere [13]. As argon atoms split under the field of photonic current in MPCVD system and electrons streams impinge such tiny grains at fixed angle, it results into their elongation as discussed in the case of gold tiny particles [4, 10], silver and binary composition of gold/silver [6] and in the case of single atom, it embedded in tiny-sized particle [11] along with oppositely existing force of two poles. Argon atoms, on splitting, shoot their electron streams to underlying matter where comprised atoms possess the feature to stretch electrons' states as per available room and opposite force of two poles. Such tiny grains are said to be elongated tiny grains and they deal modifications of their structure.

Due to process limitations, deposited carbon films in HFCVD mainly evolve in graphitic and diamond phases either increasing the content of one phase or increasing the content of one phase depending on the process conditions as discussed under varying the chamber pressure [13]. However, in MPCVD system where plentiful oxygen trapped resulting into govern the energy-directed phenomenon as well where binding of atoms is related to graphene structure where packing of paired electron states into paired unfilled electron states is south-to-north which is an opposite mechanism to diamond-diamond state atoms binding. This reveals that diamond growth is a vertical process whereas the graphene growth is a horizontal process.

Because of neutral behavior of levity gravity of electron states at bare surface, a carbon atom reveals graphitic state where an almost neutral force-directed phenomenon occurs as discussed elsewhere [13]. A carbon atom is in gas state when the pair of electron states is directed toward north-side, one electron state toward the east-side and one electron state toward the west-side. When the carbon atom is transformed into diamond state, it first gravitates the electrons to the unfilled states of neutralization at ground level under the coordination of atomic hydrogen followed by gravitating electrons under the again coordination of the atomic hydrogen to unfilled states toward the south-side of the atom and by positioning them to downward side with respect to centre of the atom (from both sides of the atom). The two forced atoms of hydrogen when coordinate to electrons (each with

each) while in their gas state carbon atom, they gravitate those electrons by bringing them to neutral state from both sides around the atom. While the forced two atoms of hydrogen further gravitate electrons of neutral state carbon atom by bringing them to downward side of south, it results into transformation of neutral state carbon atom to diamond state carbon atom. Carbon atoms in gas state, graphitic state and diamond state along with bindings of graphitic-graphitic state atoms and diamond-diamond state atoms is discussed elsewhere [13].

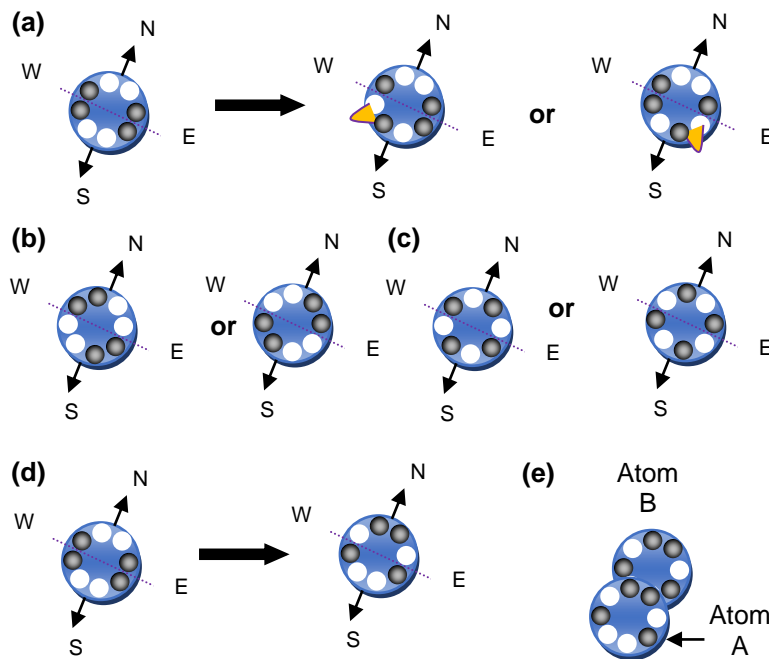


Figure 7: (a) Position of electron states (in two different options) in lonsdaleite state carbon atom on transformation of graphitic state carbon atom, (b) position of electron states (in two different options) in nanotube state carbon atom, (c) position of electron states (in two different options) in fullerene (buckyballs) state carbon atom, (d) position of electron states in graphene state carbon atom on transformation of graphitic state carbon atom and (e) binding of graphene state atoms -an energy-directed phenomenon (solid spheres denote filled electron states and white spheres unfilled ones)

The position of electron states, in two different options, in lonsdaleite state carbon atom on transformation of graphitic state carbon atom is shown in Figure 7 (a). As indicated by unit photon (force energy shape-like Gaussian distribution) along changed position of electron to its nearby unfilled state, the binding of atoms in lonsdaleite state is under force energy-directed phenomenon. In Figure 7 (b) and (c), position of electron states (in two different options) in nanotube state carbon atom and fullerene (buckyballs) carbon atom are shown where the position of electron states in their respective transformed atoms also reveal binding of atoms obey a force energy-directed phenomenon (where constructed energy knots of unit photons

bind their atoms as discussed elsewhere [9]). A force energy (unit photon) configured under the trajectory of one cycle electron's excitation/de-excitation in each atom remains burry at terminating point of inertia giving still energy knot for their binding which is a force energy-directed phenomenon. In force energy-directed phenomenon and when electrons are being excited at nearly contact distance of amalgamation of their atoms, on pulling back to nearest unfilled states available at bare surface of their atoms generated unit photons inter-crossed by retaining the right to fill dedicated unfilled state of their atoms. Position of electron states in graphene state carbon atom on transformation of graphitic state carbon atom is shown in Figure 7 (d). Binding of graphene state atoms is an energy-directed phenomenon. In energy-directed phenomenon, an electron (at target) comes to nearby unfilled state where levitated under the action of absorbed energy of that atom. In graphene atom, orientation of paired electron states is south to north under the supplied energy of oxygen atoms while evacuating from underneath surface. Through oxygen, energy supplied to atom A fixed paired electron states into conceived unfilled electron states of atom B (south to north) as shown in Figure 7 (e) where they reveal that binding of atoms in graphene is an energy-directed phenomenon. However, in the case of binding diamond-diamond state atoms, they deal a force-directed phenomenon only. An almost neutral force-directed phenomenon is involved in binding of graphitic-graphitic state atoms as discussed elsewhere [13].

Under normal condition, carbon atoms remain in the gas state and their transformations to various states depend on dealing force-, force energy-, neutral force- and energy-directed phenomena introduced by the employed conditions. In different state carbon atoms, four filled electron states and four unfilled electron states of bare surface of the atom were considered which are according to Periodic Table. The carbon atoms exhibit different states (gas, graphitic, diamond, lonsdaleite, nanotube, fullerene (bucky balls) and graphene) where master structure of a tiny grain is related to graphite structure and it is modified structure where comprised neutral state atoms deal uniform elongation (structure of smooth elements). On the other hand, tiny grains related to diamond, lonsdaleite, nanotube, fullerene (bucky balls) and graphene is related to transformed structure as resulted under the varying positions of electron states in their atoms under various directed phenomena. Graphite structure evolves under uniform electron-dynamics of atoms

where an almost neutral force-directed phenomenon enables the binding of atoms, whereas, any transformed structure evolves under non-uniform electron-dynamics of atoms where certain phenomenon (force energy-directed phenomenon or force-directed phenomenon or energy-directed phenomenon) enables the binding of atoms as given elsewhere [1].

Hardness at Mohs scale of atoms while dealing graphite structure and different transformed structure at nanoscale is sketched in Figure 8. Zero value of hardness accounts in the case of atoms when in the gas state. The hardness of graphitic state structure and various transformed structures is related to levity gravity behaviors of electron states in their atoms as depicted above. Different value of wave number of printed (recorded) intensity of energy signals (photons) from graphite structure, modified structure and various transformed structures of carbon in Raman spectroscopy reveal different trends of propagating photons under made different positions of electron states in their atoms as validated by energy loss spectroscopy as well. A diamond state of atoms never goes to corroded/oxidized state as the paired electron states of depositing atom packed to paired unfilled states of deposited atom and same is the case in graphene but is opposite to one in diamond.

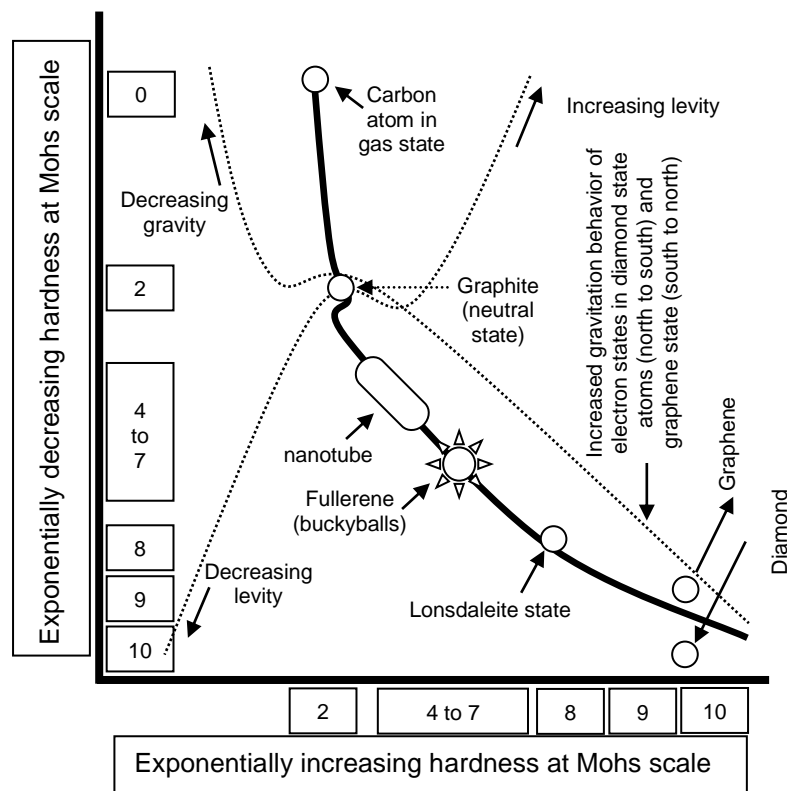


Figure 8: A sketch of approx. hardness (at Mohs scale) of various carbon allotropic forms versus allied levitation gravitation behavior available in the literature.

Our experimental studies show nearly the same width of each modified structure of smooth element along with inter-spacing distance of structure of smooth elements in gold and silver [4-8] as in the case of carbon (in Figures 3 and 4). Thus, it can be inferred that the size of each electron in the case of carbon is much bigger to what an atom owes in the case of gold or silver. This is the reason that materials based on carbon deal a very high temperature in their measurements which is again much more than what is recorded in the case of gold (or silver), well justifying the different size of their electrons. Again, the requirement of heat energy is also in the same limit when synthesizing carbon-based materials in techniques known as HFCVD, MPCVD, etc. In this context, the requirement of shunt energy to enable to free the electron at target should enhance significantly as compared to the one in silicon or in other suitable atoms of solid-state behavior.

4.0 Conclusions

'Tiny grains carbon films' synthesized under different conditions evolve graphite structure (two-dimensional structure) where it is modified to structure of smooth elements under opposite force of poles along with influence of travelling adequate energy photons. Atoms of 'tiny grains carbon films' transform into various states depending on the coordination of atomic hydrogen and oxygen. Carbon atoms transform into different states depending on the conquered position of electron states in atoms. Carbon atoms transform into graphene structure under the assistance of oxygen atoms while evacuating resulting into introduce an energy-directed phenomenon in their binding. Under the coordination of forced atomic hydrogen, positions of electron states in atoms of lonsdaleite state, nanotube state and fullerene (buckyballs) state were identified where binding of their atoms obey force energy-directed phenomenon.

Modified graphite structure tiny grains to structure of smooth elements in carbon film reveal the origin of ν_1 peak in the Raman spectrum where the lowest wave number is resulted because of enhanced field emission performance under accelerated current density rate. In the case tiny grains retain graphite structure, they reveal the origin of ν_2 peak and field emission characteristics of various known NCD/UNCD films largely depend on the ratio of ν_1 peak and ν_2 peak. Results of field emission measurements of films synthesized at different pressure are in good agreement to energy loss spectroscopy and Raman spectroscopy. In Raman

spectra, peaks related to D* band and G band are due to printed (recorded) intensities of energy signals propagated through transformed inter-state electron's gap of atoms of tiny grains into lonsdaleite state and graphene state, respectively. In energy loss spectroscopy, the peaks related to modified graphite structure tiny grains to structure of smooth elements and graphite structure are in the form of dip curves due to lower band energy as compared to the ones transformed into diamond state, lonsdaleite state and graphene state.

Our experimental results well prove and justify the position of peaks related to graphite structure, modified structure and various transformed structures of carbon in terms of wave number, band energy and field emission characteristics. In line with this, present studies set a new horizon in synthesizing, analyzing and evaluating materials at nanoscale, and soliciting reinvestigation of materials' syntheses and their performances both for existing and future applications.

Acknowledgements:

Mubarak Ali thanks National Science Council (now MOST) Taiwan (R.O.C.) for awarding postdoctorship: NSC-102-2811-M-032-008 (2013-2014). Authors wish to thank Mr. Tsung-Min Chen for assisting films' synthesis and Mr. Chien-Jui Yeh in TEM operation. Mubarak Ali greatly appreciates useful suggestions of Dr. M. Ashraf Atta and Dr. Abdul Waheed (CIIT, advisors).

References:

- [1] M. Ali, M. Ürgen, Switching dynamics of morphology-structure in chemically deposited carbon films -A new insight, Carbon 122 (2017) 653-663.
- [2] S. Link, M. A. El-Sayed, Shape and size dependence of radiative, nonradiative and photothermal properties of gold nanocrystals, Int. Rev. Phys. Chem. 19 (2000) 409- 453.
- [3] S. C. Glotzer, M. J. Solomon, Anisotropy of building blocks and their assembly into complex structures, Nature Mater. 6 (2007) 557-562.
- [4] M. Ali, I –N. Lin, The effect of the Electronic Structure, Phase Transition and Localized Dynamics of Atoms in the formation of Tiny Particles of Gold, <http://arXiv.org/abs/1604.07144>.
- [5] M. Ali, I –N. Lin, Development of gold particles at varying precursor concentration, <http://arxiv.org/abs/1604.07508>.

- [6] M. Ali, I –N. Lin, Tapping opportunity of tiny shaped particles and role of precursor in developing shaped particles, <http://arxiv.org/abs/1605.02296>.
- [7] M. Ali, I –N. Lin, Controlling morphology-structure of particles at different pulse rate, polarity and effect of photons on structure, <http://arxiv.org/abs/1605.04408>.
- [8] M. Ali, I –N. Lin, Formation of tiny particles and their extended shapes – origin of physics and chemistry of materials, <http://arxiv.org/abs/1605.09123>.
- [9] M. Ali, Structure evolution in atoms of solid state dealing electron transitions. <http://arxiv.org/abs/1611.01255>.
- [10] M. Ali, The study of tiny shaped particle dealing localized gravity at solution surface. <http://arxiv.org/abs/1609.08047>.
- [11] M. Ali, Atoms of electronic transition deform or elongate but do not ionize while inert gas atoms split. <http://arxiv.org/abs/1611.05392>.
- [12] M. Ali, Revealing the Phenomena of Heat and Photon Energy on Dealing Matter at Atomic level. <https://www.preprints.org/manuscript/201701.0028/>.
- [13] M. Ali, M. Ürgen, Dynamics of carbon atoms under varying chamber pressure while depositing films and binding of identical state atoms. (Submitted for consideration).
- [14] M. Ali, Nanoparticles-Photons: Effective or Defective Nanomedicine, J. Nanomed. Res. 5 (2017): 00139.
- [15] W. Zhu, G. P. Kochanski, S. Jin, Low-Field Electron Emission from Undoped Nanostructured Diamond, Science 282 (1998) 1471-1473.
- [16] J. Birrell, J. A. Carlisle, O. Auciello, D. M. Gruen, J. M. Gibson, Morphology and electronic structure in nitrogen-doped ultrananocrystalline diamond, Appl. Phys. Lett. 81 (2002) 2235-2237.
- [17] J. E. Dahl, S. G. Liu, R. M. K. Carlson, Isolation and Structure of Higher Diamondoids, Nanometer-Sized Diamond Molecules, Science 299 (2003) 96-99.
- [18] J. Y. Raty, G. Galli, Ultradispersity of diamond at the nanoscale, Nature Mater. 2 (2003) 792-795.
- [19] S. C. Tjong, H. Chen, Nanocrystalline materials and coatings, Mater. Sci. Engineer. R 45 (2004) 1-88.
- [20] A. V. Sumant *et al.*, Towards the Ultimate Tribological Interface: Surface Chemistry and Nanotribology of Ultrananocrystalline Diamond, Adv. Mater. 17 (2005) 1039-1045.

- [21] A. R. Krauss, O. Auciello, M. Q. Ding, D. M. Gruen, Y. Huang, V. V. Zhirnov, E. I. Givargizov, A. Breskin, R. Chechen, E. Shefer, V. Konov, S. Pimenov, A. Karabutov, A. Rakhimov, N. Suetin, Electron field emission for ultrananocrystalline diamond films, *J. Appl. Phys.* 89 (2001) 2958-2967.
- [22] X. Xiao, J. Birrell, J. E. Gerbi, O. Auciello, J. A. Carlisle, Low temperature growth of ultrananocrystalline diamond, *J. Appl. Phys.* 96 (2004) 2232-2239.
- [23] O. A. Williams, M. Nesladek, M. Daenen, S. Michaelcon, A. Hoffman, E. Osawa, K. Haenen, R. B. Jackman, Growth, electronic properties and applications of nanodiamond, *Diam. Relat. Mater.* 17 (2008) 1080-1088.
- [24] A. R. Konicek, D. S. Grierson, P. U. P. A. Gilbert, W. G. Sawyer, A. V. Sumant, R. W. Carpick, Origin of Ultralow Friction and Wear in Ultrananocrystalline Diamond, *Phys. Rev. Lett.* 100 (2008) 235502-04.
- [25] J. E. Butler, A. V. Sumant, The CVD of Nanodiamond Materials, *Chem. Vap. Deposition* 14 (2008) 145-160.
- [26] J. P. Thomas, H. C. Chen, N. H. Tai, I -N. Lin, Freestanding Ultrananocrystalline Diamond Films with Homo Junction Insulating Layer on Conducting Layer and Their High Electron Field Emission Properties, *ACS Appl Mater Interfaces* 3 (2011) 4007-4013.
- [27] W. Kulisch, C. Petkov, E. Petkov, C. Popov, P. N. Gibson, M. Veres, R. Merz, B. Merz, J. P. Reithmaier, Low temperature growth of nanocrystalline and ultrananocrystalline diamond films: A comparison, *Phys. Status Solidi A* 209 (2012) 1664-1674.
- [28] K. J. Sankaran *et al.*, Improvement in plasma illumination properties of ultrananocrystalline diamond films by grain boundary engineering, *J. Appl. Phys.* 114 (2013) 054304-11.
- [29] K. J. Sankaran *et al.*, Improvement in Tribological Properties by Modification of Grain Boundary and Microstructure of Ultrananocrystalline Diamond Films, *ACS Appl. Mater. Interfaces* 5 (2013) 3614-3624.
- [30] A. Saravanan *et al.*, Fast growth of ultrananocrystalline diamond films by bias-enhanced nucleation and growth process in CH₄/Ar plasma, *Appl. Phys. Lett.* 104 (2014) 181603-5.
- [31] C. S. Wang, H. C. Chen, H. F. Cheng, I -N. Lin, Origin of platelike granular structure for the ultrananocrystalline diamond films synthesized in H₂ - containing Ar / CH₄ plasma, *J. Appl. Phys.* 107 (2014) 034304-7.

- [32] H. Zeng *et al.*, Boron-doped ultrananocrystalline diamond synthesized with an H-rich/Ar-lean gas system, *Carbon* 84 (2015) 103-117.
- [33] K. J. Sankaran, K. Panda, B. Sundaravel, H. –C. Chen, I –N. Lin, C. –Y. Lee, N. –H. Tai, Engineering the Interface Characteristics of Ultrananocrystalline Diamond Films Grown on Au-Coated Si Substrates, *ACS Appl. Mater. Interfaces* 4 (2012) 4169-4176.
- [34] J. P. Thomas *et al.*, Preferentially Grown Ultrananocrystalline c-Diamond and n-Diamond Grains on Silicon Nanoneedles from Energetic Species with Enhanced Field-Emission Properties, *ACS Appl. Mater. Interfaces* 4 (2012) 5103-5108.
- [35] K. J. Sankaran, H. –C. Chen, K. Panda, B. Sundaravel, C. –Young Lee, N. –H. Tai, I –N. Lin, Enhanced Electron Field Emission Properties of Conducting Ultrananocrystalline Diamond Films after Cu and Au Ion Implantation, *ACS Appl. Mater. Interfaces* 6 (2014) 4911-4919.
- [36] K. J. Sankaran, K. Panda, B. Sundaravel, N. H. Tai, I –N. Lin, Enhancing electrical conductivity and electron field emission properties of ultrananocrystalline diamond films by copper ion implantation and annealing, *J. Appl. Phys.* 115 (2014) 063701-7.
- [37] K. J. Sankaran *et al.*, Electron Field Emission Enhancement of Vertically Aligned Ultrananocrystalline Diamond-Coated ZnO Core–Shell Heterostructured Nanorods, *Small* 10 (2014) 179-185.
- [38] Y. Tzeng, S. Yeh, W. C. Fang, Y. Chu, Nitrogen-incorporated ultrananocrystalline diamond and multi-layer-graphene-like hybrid carbon films, *Sci. Rep.* 4 (2014) 4531.
- [39] S. C. Lin *et al.*, The microstructural evolution of ultrananocrystalline diamond films due to P ion implantation and annealing process-dosage effect, *Diam. Relat. Mater.* 54 (2015) 47-54.
- [40] K. Panda, E. Inami, Y. Sugimoto, K. J. Sankaran, I –Nan Lin. Straight imaging and mechanism behind grain boundary electron emission in Pt-doped ultrananocrystalline diamond films. *Carbon* 111 (2017) 8-17.
- [41] A. Saravanan, B. R. Huang, K. J. Sankaran, G. Keiser, J. Kurian, N. H. Tai, I. N. Lin, Structural modification of nanocrystalline diamond films via positive/negative bias enhanced nucleation and growth processes for improving their electron field emission properties, *J. Appl. Phys.* 117 (2015) 215307-11.

- [42] D. M. Gruen, S. Liu, A. R. Krauss, X. Pan, Buckyball microwave plasmas: Fragmentation and diamond-film growth, *J. Appl. Phys.* 75 (1994) 1758-1763.
- [43] P. Kovarik, E. B. D. Bourdon, R. H. Prince, Electron-energy-loss characterization of laser-deposited *a*-C, *a*-C:H, and diamond films, *Phys. Rev. B* 48 (1993) 12123-12129.
- [44] W. A. Yarbrough, R. Messier, Current issues and problems in the chemical vapor deposition of diamond, *Science* 247 (1990) 688-696.
- [45] R. J. Nemanich, J. T. Glass, G. Lucovsky, R. E. Shroder, Raman scattering characterization of carbon bonding in diamond and diamondlike thin films, *J. Vac. Sci. Technol. A* 6 (1988) 1783-1787.
- [46] R. E. Shroder, R. J. Nemanich, J. T. Glass, Analysis of the composite structures in diamond thin films by Raman spectroscopy, *Phys. Rev. B* 41 (1990) 3738-3745.
- [47] A. C. Ferrari, J. Robertson, Origin of the 1150cm^{-1} Raman mode in nanocrystalline diamond, *Phys. Rev. B* 63 (2001) 121405-5.
- [48] I. Jiménez, M. M. García, J. M. Albella, L. J. Terminello, Orientation of graphitic planes during the bias-enhanced nucleation of diamond on silicon: An x-ray absorption near-edge study, *Appl. Phys. Lett.* 73 (1998) 2911-2913.
- [49] J. Birrell, J. E. Gerbi, O. Auciello, J. M. Gibson, J. Johnson, J. A. Carlisle, Interpretation of the Raman spectra of ultrananocrystalline diamond, *Diam. Relat. Mater.* 14 (2005) 86-92.
- [50] R. Haubner, M. Rudigier, Raman characterisation of diamond coatings using different laser wavelengths, *Physics Procedia* 46 (2013) 71-78.
- [51] S. C. Ray, I -N. Lin, Ferroelectric behaviours of ultra-nano-crystalline diamond thin films, *Surf. Coat. Technol.* 271 (2015) 247-250.

Authors' biography:

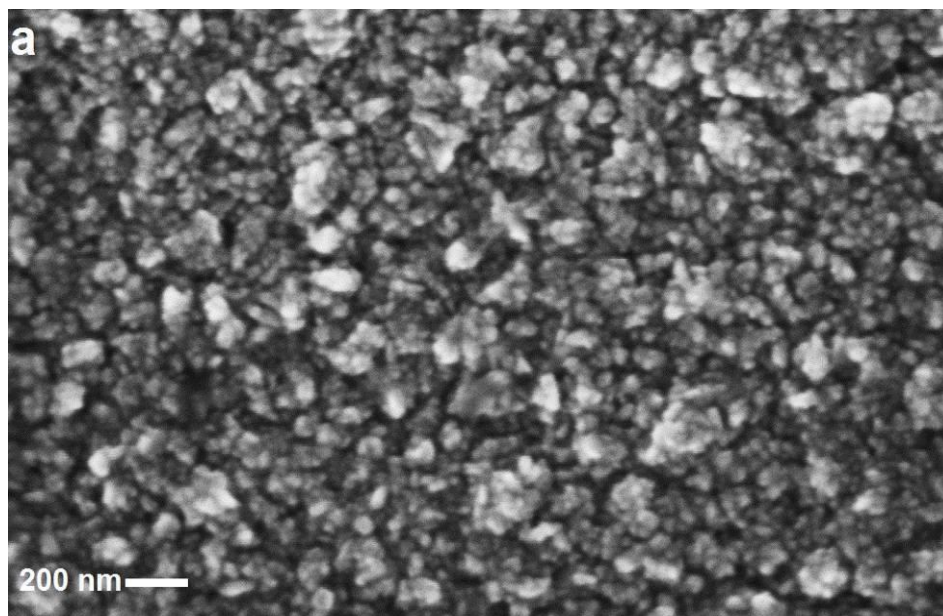


Mubarak Ali graduated from University of the Punjab with B.Sc. (Phys& Maths) in 1996 and M.Sc. Materials Science with distinction at Bahauddin Zakariya University, Multan, Pakistan (1998); thesis work completed at Quaid-i-Azam University Islamabad. He gained Ph.D. in Mechanical Engineering from Universiti Teknologi Malaysia under the award of Malaysian Technical Cooperation Programme (MTCP;2004-07) and postdoc in advanced surface technologies at Istanbul Technical University under the foreign fellowship of The Scientific and Technological Research Council of Turkey (TÜBİTAK; 2010). He completed another postdoc in the field of nanotechnology at Tamkang University Taipei (2013-2014) sponsored by National Science Council now M/o Science and Technology, Taiwan (R.O.C.). Presently, he is working as Assistant Professor on tenure track at COMSATS Institute of Information Technology, Islamabad campus, Pakistan (since May 2008) and prior to that worked as assistant director/deputy director at M/o Science & Technology (Pakistan Council of Renewable Energy Technologies, Islamabad; 2000-2008). He was invited by Institute for Materials Research (IMR), Tohoku University, Japan to deliver scientific talk on growth of synthetic diamond without seeding treatment and synthesis of tantalum carbide. He gave several scientific talks in various countries. His core area of research includes materials science, physics & nanotechnology. He was also offered the merit scholarship (for PhD study) by the Government of Pakistan but he couldn't avail. He is author of several articles published in various periodicals (<https://scholar.google.com.pk/citations?hl=en&user=UYivhDwAAAAJ>).



I-Nan Lin is a senior professor at Tamkang University, Taiwan. He received the Bachelor degree in physics from National Taiwan Normal University, Taiwan, M.S. from National Tsing-Hua University, Taiwan, and the Ph.D. degree in Materials Science from U. C. Berkeley in 1979, U.S.A. He worked as senior researcher in Materials Science Centre in Tsing-Hua University for several years and now is faculty in Department of Physics, Tamkang University. Professor Lin has more than 200 referred journal publications and holds top position in his university in terms of research productivity. Professor I-Nan Lin supervised several PhD and Postdoc candidates around the world. He is involved in research on the development of high conductivity diamond films and on the transmission microscopy of materials.

Supplementary Materials:



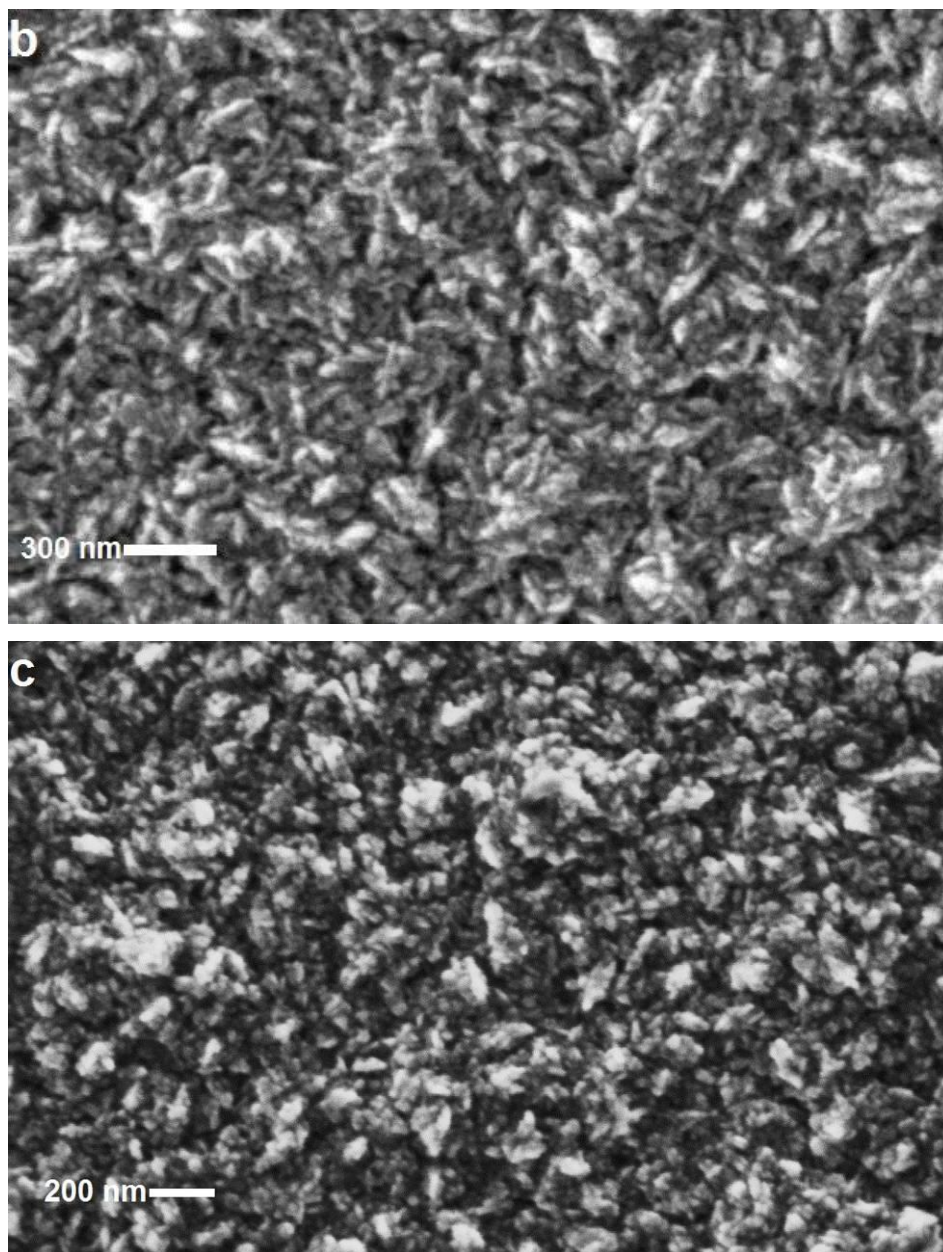


Figure S1: Surface morphology of 'tiny grains carbon films' synthesized at chamber pressure (a) 100 torr, (b) 150 torr, and (c) 200 torr; total mass flow rate: 200 sccm (6% H₂, 1 % CH₄ and 93 % argon, Ar: CH₄: H₂ = 186:2:12), microwave power: 1400 (in watts) and deposition time: 60 minutes.

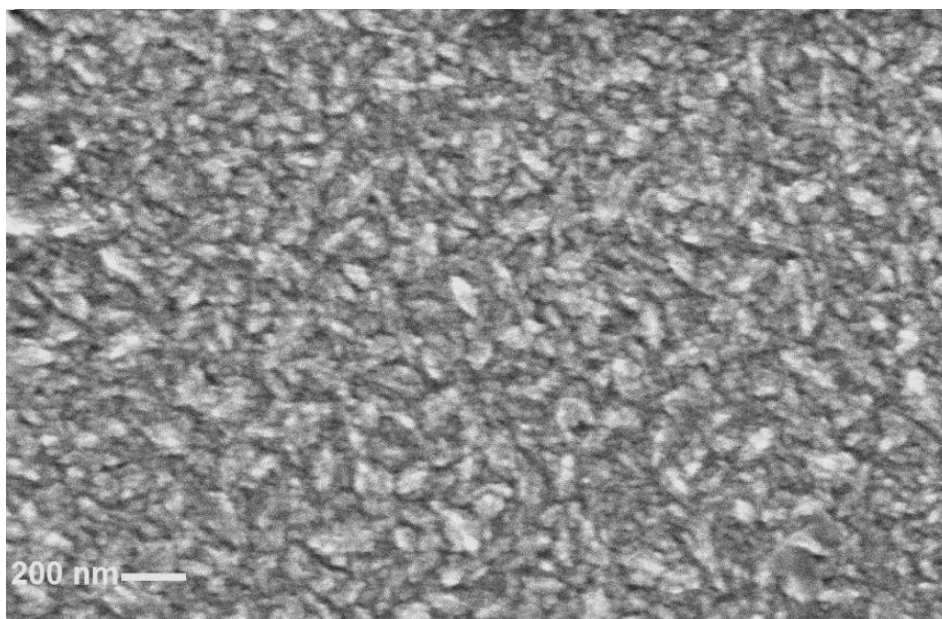


Figure S2: Surface morphology of 'tiny grains carbon film' synthesized at chamber pressure 150 torr; total mass flow rate: 200 sccm (0% H₂, 2 % CH₄ and 98 % argon, Ar: CH₄: H₂ = 196:4:0), microwave power: 1100 (in watts) and deposition time: 60 minutes.

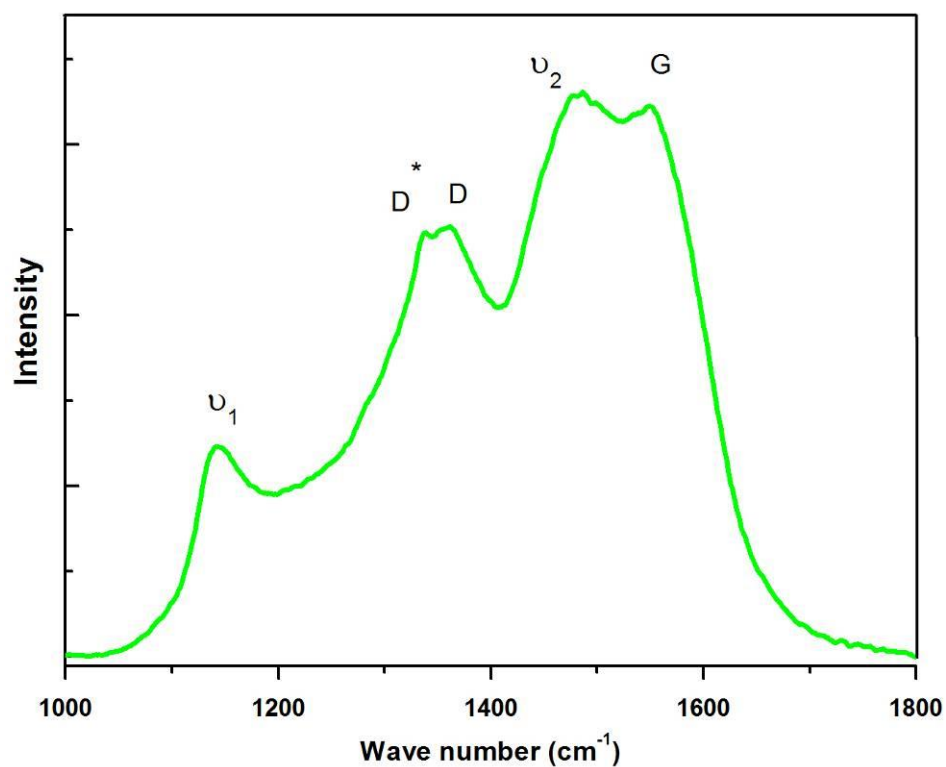
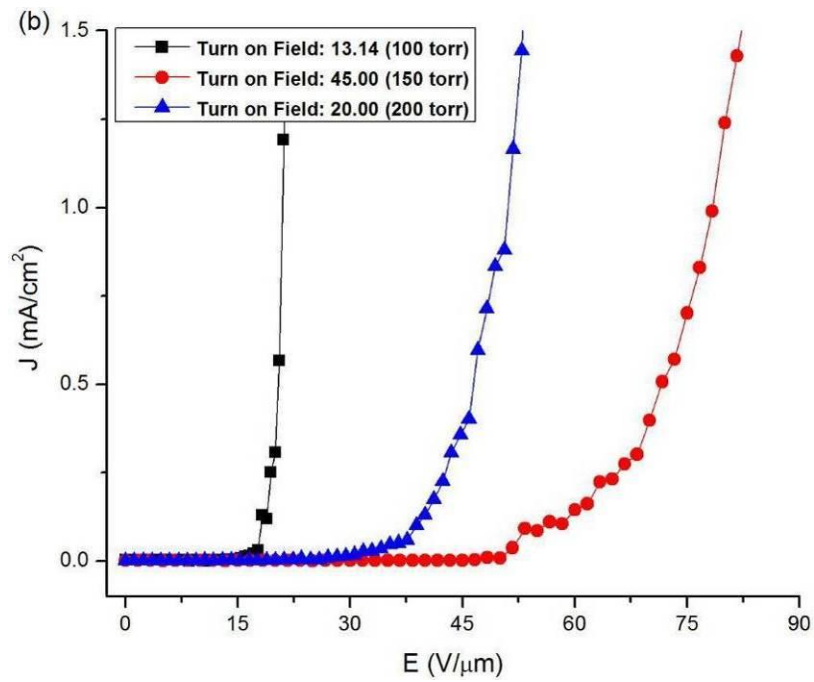
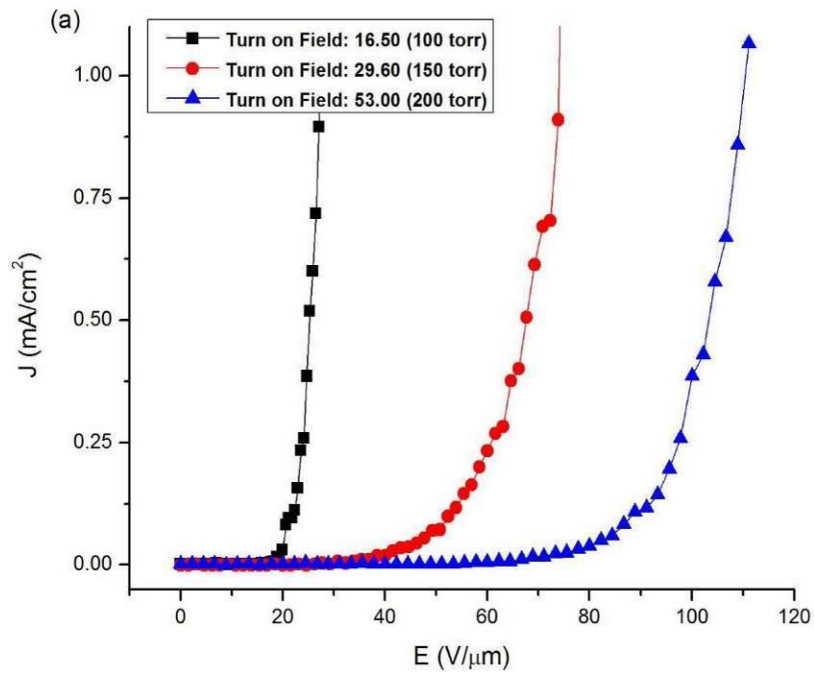


Figure S3: Raman spectrum of 'tiny grains carbon film' synthesized at chamber pressure 150 torr; total mass flow rate: 200 sccm (0% H₂, 2 % CH₄ and 98 % argon, Ar: CH₄: H₂ = 196:4:0), microwave power: 1100 (in watts) and deposition time: 60 minutes (v₁: ~ 1145 cm⁻¹, D*: ~ 1310 cm⁻¹, D: 1332 cm⁻¹, v₂: ~ 1480 cm⁻¹, G: ~ 1580 cm⁻¹).



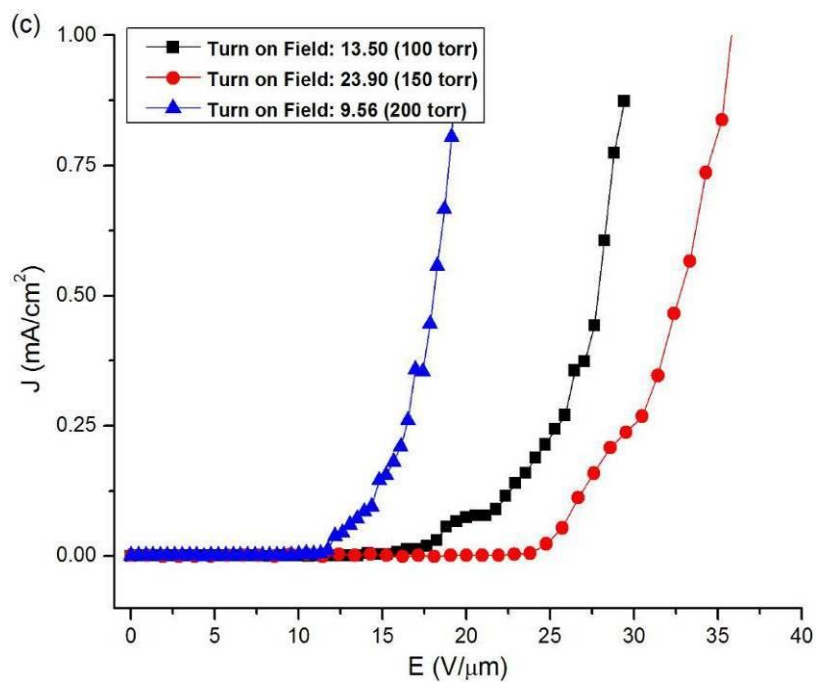
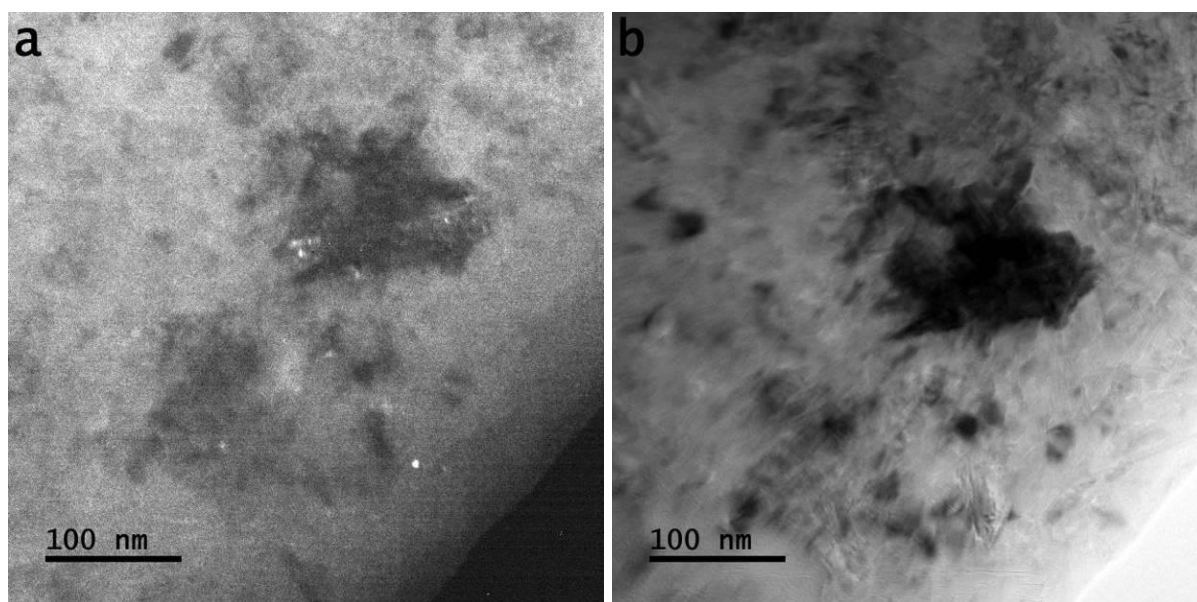


Figure S4: Field emission current density as a function of applied field of 'tiny grains carbon films' synthesized (a) without H₂, (b) with 3 % H₂ and (c) with 6 % H₂; 1 % CH₄, total mass flow rate: 200 sccm, microwave power: 1200 (in watts) and deposition time: 60 minutes.



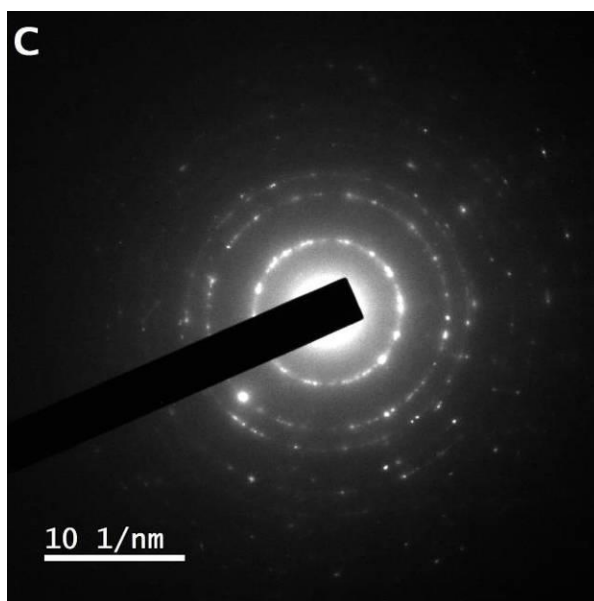
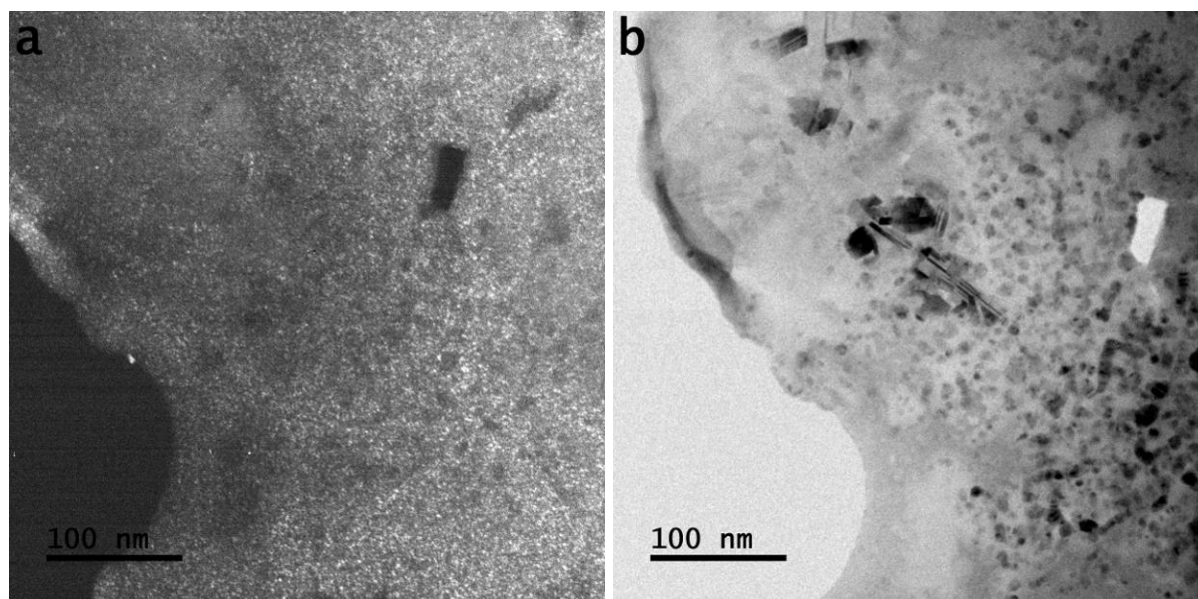


Figure S5: (a) Dark field transmission microscope image (b) bright field transmission microscope image and (c) SAPR pattern of 'tiny grains carbon film' synthesized at chamber pressure: 100 torr, total mass flow rate: 200 sccm (6% H₂, 1 % CH₄ and 93 % argon), microwave power: 1400 watts (in watts) and deposition time: 60 minutes.



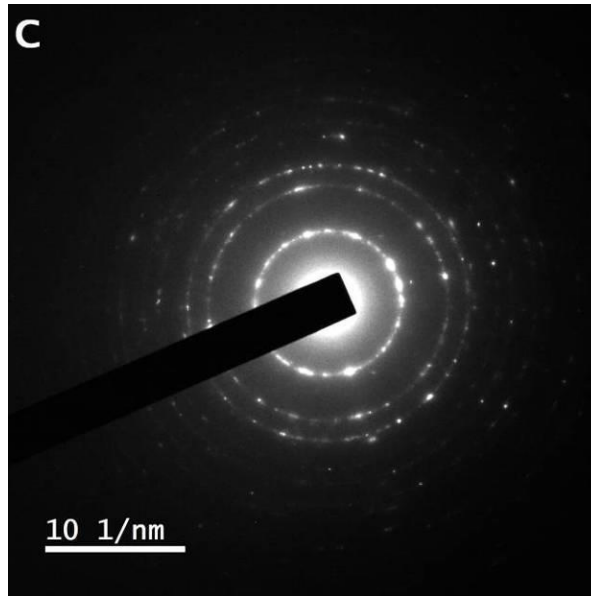


Figure S6: (a) Dark field transmission microscope image (b) bright field transmission microscope image and (c) SAPR pattern of 'tiny grains carbon film' synthesized at chamber pressure: 200 torr, total mass flow rate: 200 sccm (6% H₂, 1 % CH₄ and 93 % argon), microwave power: 1400 (in watts) and deposition time: 60 minutes.

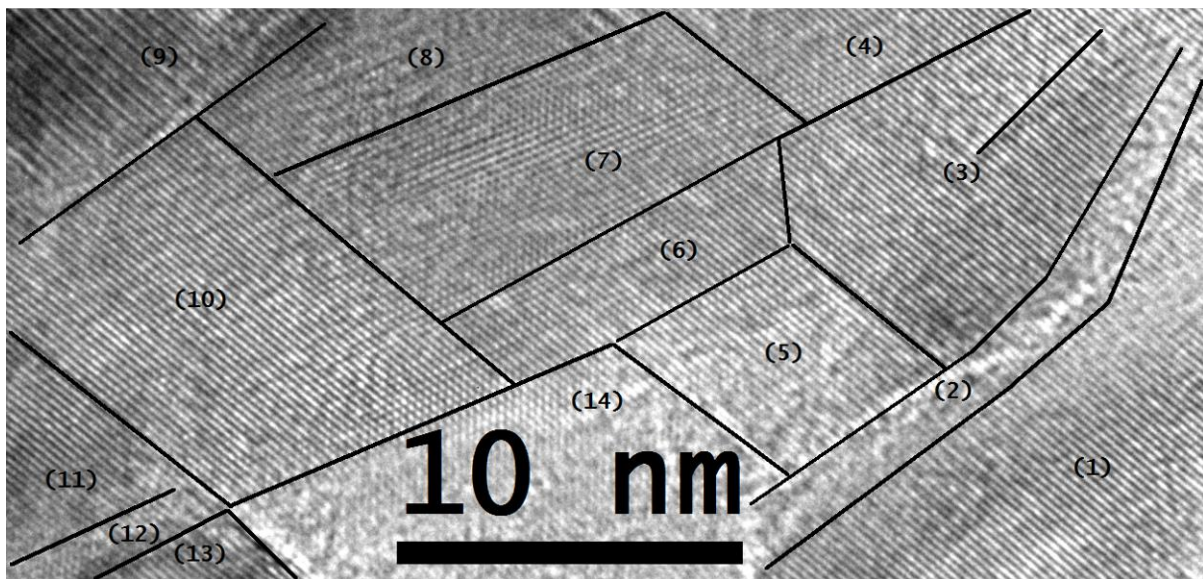


Figure S7: High-resolution transmission microscope image of 'tiny grains carbon film' synthesized at chamber pressure 100 torr shows graphite structure, modified structure and different transformed structures of atoms/tiny grains; total mass flow rate: 200 sccm (6% H₂, 1 % CH₄ and 93 % argon), microwave power: 1400 (in watts) and deposition time: 60 minutes.